Density Functional Theory Investigation of Intermolecular Interactions for Hydrogen-Bonded Deep Eutectic Solvents

B. Myrzakhmetov[1,2], M. Karibayev[1], Y. Wang[1,3], A. Mentbayeva[1,2]*

[1]Department of Chemical and Materials Engineering, School of Engineering and Digital Sciences,
Nazarbayev University, Kabanbay Batyr ave. 53, Astana, Kazakhstan
[2]Laboratory of Energy Storage Systems, Center for Energy and Advanced Materials Science, National Laboratory Astana,
Nazarbayev University, Kabanbay Batyr ave. 53, Astana, Kazakhstan
[3]Laboratory of Computational Materials Science for Energy Applications, Center for Energy and Advanced Materials
Science, National Laboratory Astana, Nazarbayev University, Kabanbay Batyr ave. 53, Astana, Kazakhstan

Article info

Abstract

Examining the interplay between choline chloride (ChCl) and ethylene glycol (EG) in Deep Eutectic Solvents (DES) assumes a pivotal role in designing innovative solvents. According to the literature, the comprehensive analysis of all possible types of conformers of ChCl and EG-based DES was scarce at different ratios, highlighting a gap in understanding at the atomistic level. In this study, we address this gap through a detailed Density Functional Theory calculation with dispersion correction (DFT+D3). Employing Density Functional Theory (DFT) calculations, our investigation delves into intermolecular relationships within DES, particularly focusing on ChCl and EG-based DES. DFT outcomes highlight the 1:2 ChCl to EG based DES ratio as notably more stable than alternative conformers. Key interactions within this DES conformation include: i) choline-chloride charge centers, ii) choline-EG links, and iii) EG-chloride anion associations. These findings provide valuable insights for crafting advanced solvents with tailored attributes. The intricate intermolecular interplay demonstrated here offers a versatile framework for harnessing DES potential across various domains, from chemical engineering to sustainable technologies.

Abbreviations

DES – Deep eutectic solvent
DFT – Density functional theory calculation
DFT+D3 – Density functional theory with dispersion correction
IL – Ionic liquid
HBD – Hydrogen bond donor
HBA – Hydrogen bond acceptor
MD – Molecular dynamic simulation
MEP – Molecular electrostatic potential map
HOMO – Highest occupied molecular orbital
LUMO – Lowest unoccupied molecular orbital
RDG – Reduced density gradient

ELF – Electron localized function
$\Delta E_{binding}$ – Binding energy
BSSE – Basis set superposition error
ChCl – Choline chloride
EG – Ethylene glycol
AIM – Atom in molecule theory
NCI – Non-covalent interaction

1. Introduction

In recent years, as prospective substitutes for water as the electrolyte in membranes, non-volatile and conductive solvents like ionic liquids (ILs) and deep eutectic solvents (DESs) have thus attracted substantial attention [1–3]. DESs are new family of green ILs that consist of hydrogen bond donors (HBDs) and hydrogen bond acceptors (HBAs) [4, 5].

*Corresponding author.
E-mail address: almagul.mentbayeva@nu.edu.kz

Due to the hydrogen bonding between HBD and HBA, they are homogenous and have a lower melting point [6, 7]. In addition to having a lower melting temperature than their components, DESs also benefit from non-toxicity, low viscosity, accessibility, and ease of synthesis [8, 9]. These favorable characteristics make them suitable candidates as solvents in various processes, such as polymer production, separation media for gas mixtures, and enzyme activators and stabilizers [10]. The predictive power of structure-property connections provided by computer modeling can significantly reduce the time and resources used in empirically improving such systems [11]. As a result, many studies [12–14] have described various methods, including density functional theory (DFT) calculations and molecular dynamic (MD) simulations, to provide some insight into the structure and interactions essential in eutectic liquids. Due to complex supramolecular structures in DESs created by hydrogen bonding, the theoretical investigation of DESs captured the interest. In addition, theoretical modeling can offer a dynamic tool to simulate molecular graphics and physico-chemical characteristics [15]. MD simulations have been used to examine the structural characteristics of two deep eutectic solvents, namely a 1:2 mixture of butyltrimethylammonium chloride and urea and a 1:2 mixture of choline chloride (ChCl) and urea [16]. It has been discovered that the DESs' hydrogen bond network is significantly impacted by whether an organic cation contains a hydroxyl group or not, leading to a different three-dimensional arrangement of all the species present in the mixtures. These results may significantly affect how developed DESs are going forward for particular applications [17]. According to Carriazo et al. and Zahn et al., the charge delocalization that results from hydrogen bonding between the halide anion and the hydrogen-donor moiety causes the mixture's freezing point to drop relative to the melting points of its constituent parts [18, 19]. However, a practical or theoretical demonstration still needs to be improved. Therefore, the DFT method has been used in this study to analyze the structural, physical, and electronic characteristics of hydrogen-bonded supramolecular structures. These results would be helpful in exploring the use of these solvents in the electrochemical area and for understanding the hydrogen-bonded supramolecular structure of DESs and other related properties.

In this study, DFT calculations with dispersion correction (DFT+D3) were performed to investigate the intermolecular interactions of ChCl with ethylene glycol (EG) based DES. Typical and commonly used DES including ChCl with EG was selected as theoretical models for DFT calculations. In the following paragraphs, DFT calculation methodology, and quantum chemical properties for DES was described and discussed.

2. Model and Method

2.1 System of interest

The ChCl with EG based DESs structure was designed in ratios 1:1 and 1:2 (Fig. 1A, B), to create the computational models of DES for DFT calculations.
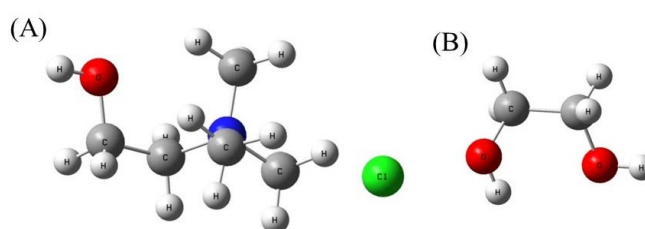

Fig. 1. Structure of DES components including (A) ChCl, and (B) EG.

2.2 DFT + D3 calculations

DFT+D3 calculations were used to optimize the electronic ground state geometries, as well as to obtain molecular electrostatic potential (MEP) maps, bond length, distribution of LUMO and its energy, critical points, non-covalent interactions (NCI), reduced density gradient (RDG), electron localization function (ELF), topology analysis, binding energy ($\Delta E_{binding}$). DFT with B3LYP functional was applied to optimize the DES [20, 21]. To determine the MEP, LUMO distribution, LUMO energies, critical points, NCI, RDG, ELF, topology analysis, and $\Delta E_{binding}$ for typical DES, B3LYP 6-311++G(2d,p) with basis set superposition error (BSSE) DFT+D3 calculations were performed [22, 23]. Herein, $\Delta E_{binding}$ was estimated using the variations in total energy values of the DES and constituent components of DES were present, as given in Eq. (1).

$$\Delta E_{binding} = E_{AB} - (E_A + E_B) + BSSE \qquad (1)$$

All stationary locations were proved to be absolute minima on their respective potential energy surfaces by further computations of the second energy derivatives. The GaussView (v6.0) program (Gaussian, Inc., Wallingford CT), GAUSSIAN16, and Multiwfn software were adopted for all DFT+D3 calculations and analysis [24, 25].
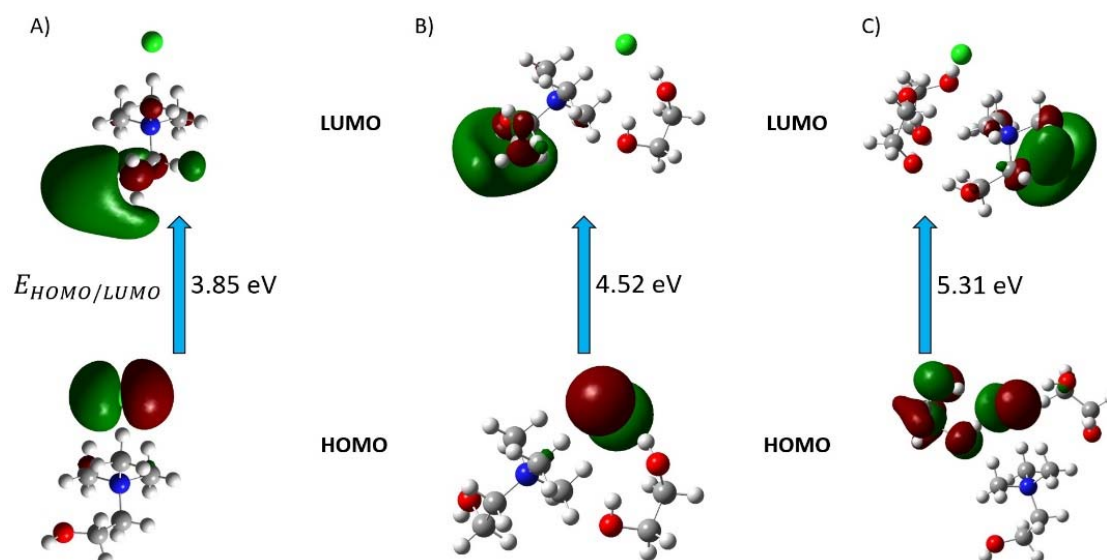
Fig. 2. $\Delta E_{binding}$ values for ten different conformers of DES.

3. Results and discussion

This section's DFT+D3 calculation results discuss the intermolecular interactions of DES components. Major analyses and discussions are focused on the study of quantum chemical features, such as $\Delta E_{binding}$, optimized structures, critical points, NCI, RDG, electron density, ELF, and MEPs.

3.1 Binding energies

In order to study the most stable molecular structure of the DES conformers in 1:1 and 1:2 ratios, values of binding energies were obtained via DFT+D3 calculations. The selected ten possible molecular structural conformers of DES, with the binding energies, are presented in Fig. 2. As a result of DFT calculations, the improvement in the binding energy value in DES conformer is due to the formation of new thermodynamically favored intermolecular interactions between ChCl and the EG components.

This is better highlighted in DES3, DES4, DES5, DES8, DES9, and DES10 conformers that both acidic hydrogens of hydroxyl groups of ethylene glycol molecules and hydroxyl group of ChCl mediate better interactions with the chloride to form one or more hydrogen bonds in comparison with other DES1, DES2, DES6, and DES7 conformers as can be seen in Fig. 2. This is consistent with the findings of others in the literature.

3.2 Optimized structures

The intermolecular interactions in pure ChCl and in DES conformer (i) (previously mentioned as DES4) were illustrated in Fig. 3 for a better comparison of intermolecular interaction changes for ChCl before and after mixing with EG to form DES. As a result, it can be noted that, the distances between chloride ion and acidic hydrogen atoms of choline were 2.35, 2.45, and 2.36 Angstrom respectively. After mixing ChCl with EG, the chloride ion acts as a hydrogen bond acceptor and interacts with acidic hydrogen atoms of EG as well.

In detail, the primary interactions in DES conformer (i) are formed as follows: i) between the choline and chloride charge centers, ii) between the choline and EG, and iii) between the EG and the chloride anion. For example, the distance between chloride ion and hydrogen atoms of choline was 2.69, 2.53, and 2.58 Angstroms, while the hydrogen bond distance between chloride ion and hydrogen atoms of EG was 2.36, 2.25, 2.23, and 3.17 Angstroms respectively as shown in Fig. 3.

Fig. 3. Optimized structure of ChCl and DES conformer (i).

Fig. 4. HOMO-LUMO gap of ChCl (A), ChCl:EG 1:1 (B) and 1:2 ratio (C).

3.3 Frontier molecular orbital analysis

The HOMO and LUMO are key electronic states in a molecule, representing the highest occupied (HOMO) and lowest unoccupied (LUMO) molecular orbitals, respectively. The HOMO-LUMO energy gap provides valuable information about the electronic structure and properties of a molecule, and it has implications for various aspects of its behavior. Larger HOMO-LUMO gaps generally indicate greater kinetic stability and chemical inertness. In contrast, smaller gaps often suggest higher reactivity. The stability order of the studied compounds is given as ChCl:EG 1:2 > ChCl:EG 1:1 > ChCl as shown in Fig. 4.

Calculated results suggest that DES based on ChCl:EG with 1:2 ratio has the highest stability, while compound ChCl has the lowest. the discussion indicates that the electron accepting ability of the groups in the studied compounds plays a significant role in determining their stability, and this is reflected in the LUMO-HOMO energy gap, global hardness, and chemical reactivity of the compounds.

3.4 Critical points

More analyses on the selected DES conformer (i) was carried out using the Bader's atom in molecule (AIM) theory. In Fig. 5, the critical points related to the pure ChCl and DES component (i) are presented. Based on the AIM theory, critical point between each pair of nuclei is considered as "bond". From Fig. 5, it is obvious that, in addition to the regular bonds, other critical points are noticeable. Three of them are related to the acidic hydrogens of choline and chloride ion.

These interactions, based on the electronegativity of the elements, can be considered as the hydrogen bonding. The other three are related to the interaction between acidic hydrogens of hydroxyl groups of EG and chloride ion. To shed a light on this observation, further quantum chemical analysis was performed.

3.5 Non covalent interactions

Considering the mentioned results, additional analysis is needed to conclude the identity of the observed interactions. Herein, the NCI analysis for ChCl and DES conformer (i) was noted in Fig. 6.

As a result, the Van der Waals interactions have very small electron density in the region between chloride and choline, while in the strong steric interactions or hydrogen bonds, a relatively large amount of electron density is visible noted in the region between chloride ion and EG molecule.
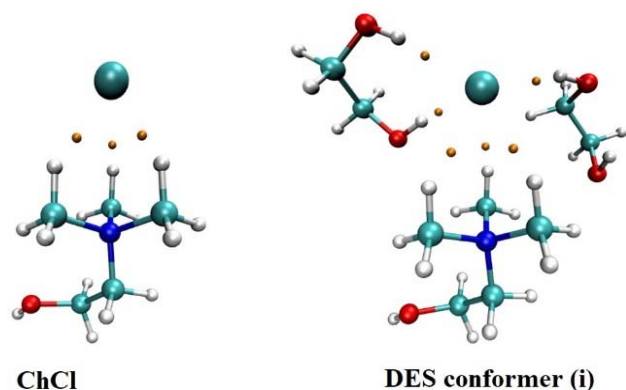

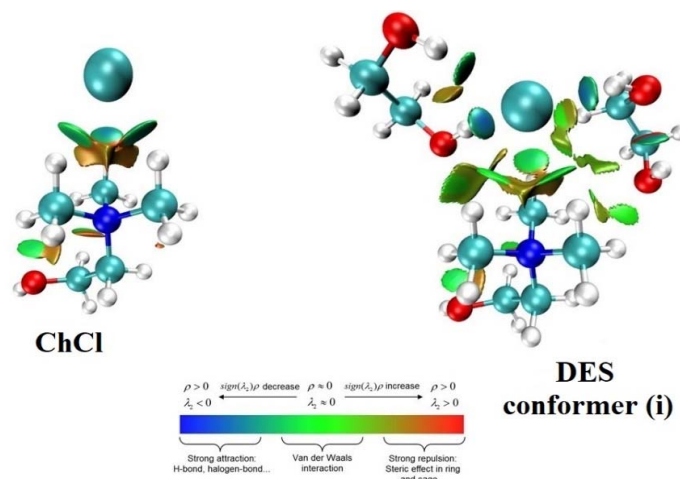**Fig. 5.** Critical points for ChCl and DES conformer (i).

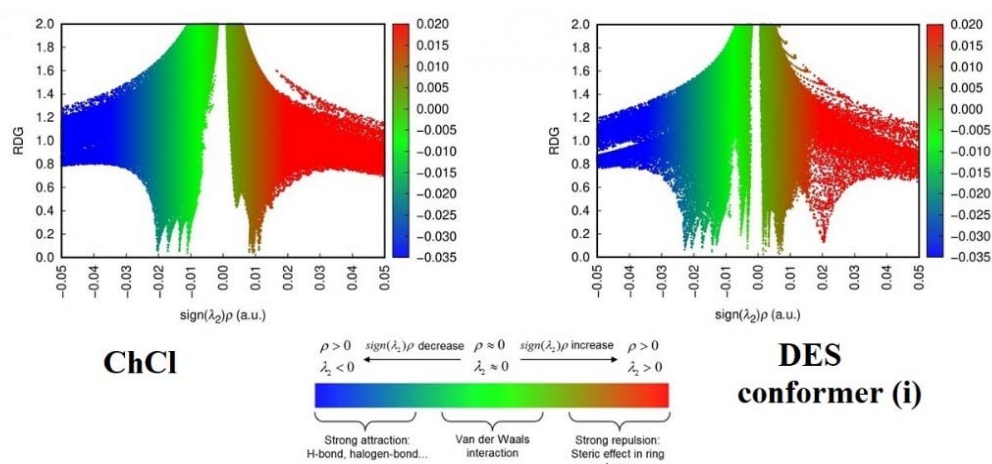**Fig. 6.** NCI in ChCl and DES conformer (i).

Fig. 7. RDG of ChCl and DES conformer (i).

3.6 Reduced density gradient

The RDG is used to characterize the strength of the electron-electron interactions in a molecular system. It provides information about regions of high electron density and helps identify regions where noncovalent interactions, such as hydrogen bonding or van der Waals interactions, may occur as can be seen in Fig. 7.

The color-coded visualization identifies different types and strengths of molecular interactions in the ChCl and DES conformed (i) systems. The cyan line indicates the presence of conventional hydrogen bonds which are intense and higher in DES, while the transition region suggests van der Waals inter-*actions.*

3.7 Electron density plot

Electron density plots are used to visualize the charge distribution of molecules. Electron density plots show the amount of electron density at each point in the molecule. This is represented by a color scale, with red indicating high electron density and blue indicating low electron density. Electron density plots can be used to see where the electrons are concentrated in a molecule, which can help to understand the bonding patterns as can be seen in Fig. 8.

From the results of Fig. 8, it can be noted that higher electron density is located at around chloride ion, and nitrogen, carbon atoms of choline in pure ChCl. While this trend was changed in DES conformer (i), where high electron density is noted around oxygen atoms of EG. In general, electron density plots are more useful for understanding the bonding patterns of molecules.

3.8 Electron localization function

Next, the ELF and localized orbital locators were calculated to visualize the nature of the bonds as can
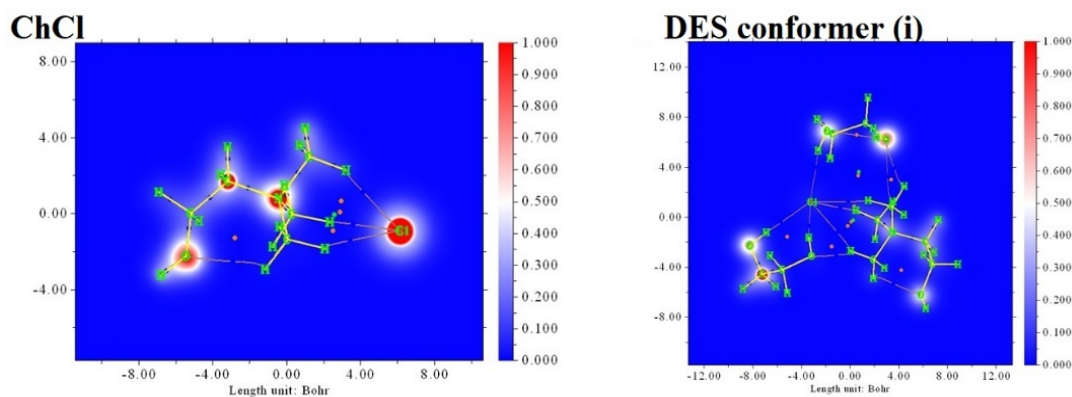
Fig. 8. Electron density of ChCl and DES conformer (i).

be seen in Fig. 9. ELF maps are useful tools to distinguish between chemical bonding (shared-electron interactions, i.e., covalent bonds) and physical bonding (i.e., ionic, hydrogen, and Van der Waals, with unshared-electron interactions) in simple molecular systems; moreover, the strength of the interaction depends on the ELF profile.

A higher value of ELF, $n(r) > 0.7$, is representative of a stronger shared-electron interaction, where electrons are localized. Covalent bonds in molecules are detected, setting a value of $n = 0.88$. Instead, in hydrogen bonds, no shared electrons are localized in the regions between the molecules, but they can be visualized by the vicinity of their respective basins that sometimes are even touching, in the case of stronger hydrogen bonds, with n values around 0.3–0.2.

3.9 Electrostatic potential maps

Electrostatic potential maps are used to visualize the charge distribution of molecules as can be seen in Fig. 10. Electrostatic potential maps show the electrostatic potential energy at each point in the molecule. This is the potential energy that a positive test charge would experience at that point. Herein, red indicates low electrostatic potential energy and blue indicates high electrostatic potential energy.

Electrostatic potential maps can be used to see where the positive and negative charges are located in a molecule, which can help to understand the polarity of the molecule and its interactions with other molecules. Herein, the negative charges can be noted around chloride ion, and oxygen atoms of
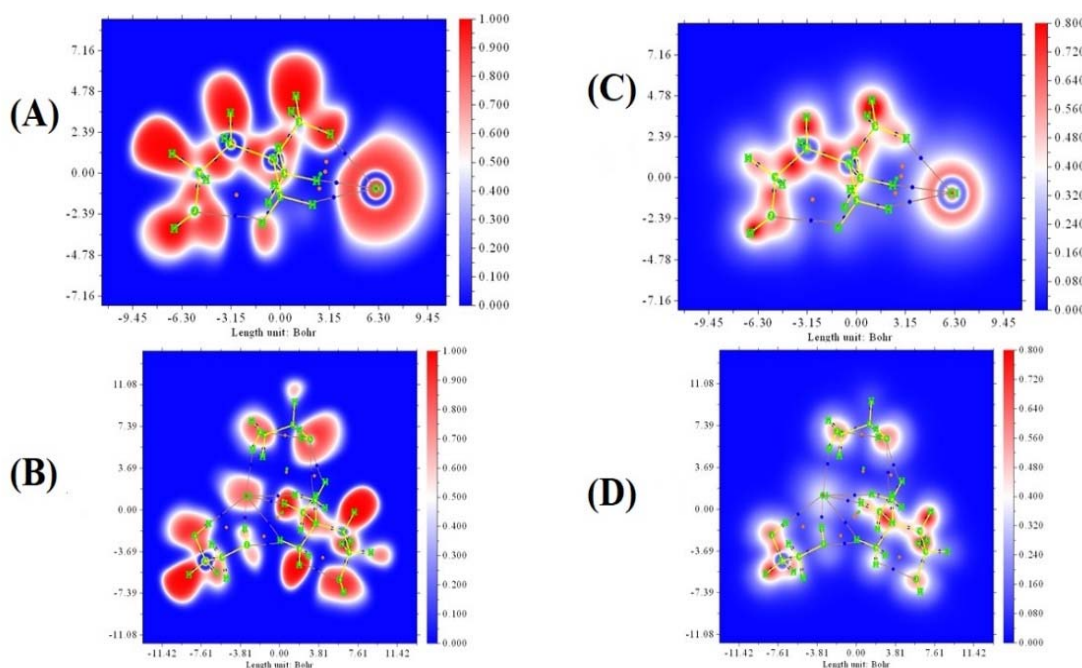
Fig. 9. ELF (A,B) and localized orbital locator (C, D) of ChCl (A, C) and DES conformer (i) (B, D).
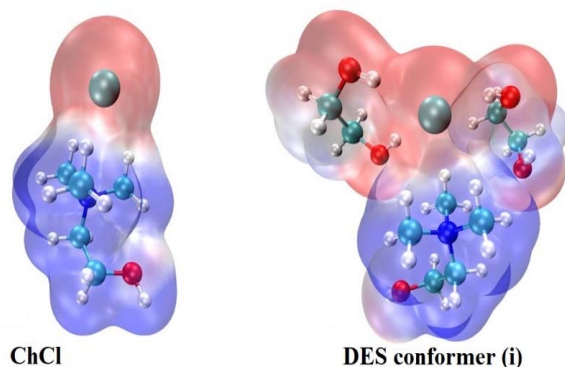
Fig. 10. Electrostatic potential maps of ChCl and DES conformer (i).

ethylene glycol, while positive charges were located around the nitrogen atoms of choline.

In the literature, several experimental studies have been conducted on the synthesis and characterization of ChCl:EG based DES [25–29]. These studies reported a measured density, surface tension, refractive index, and others [29]. Additionally, Perkins et al. conducted experimental and computational work, revealing a higher number of hydrogen bonds between ChCl-based DES molecules [30]. They also identified two close contacts: one between the chlorine anion and the hydroxyl hydrogen atom of choline, and the other between the anion and the hydroxyl hydrogen atoms in ethylene glycol [30]. These findings align well with our own observations.

DESs are classified based on their constituents, hydrophilicity, hydrogen bond donor/acceptor ratio (HBD/HBA), properties, and applications. Our ChCl/EG based DES demonstrates a wide range of applications, serving as membrane support materials in Proton Exchange Membrane Fuel Cells (PEMFC), a solvent for the recovery of cobalt from lithium-ion batteries through recycling processes, and in various other areas [31–33]. This study not only contributes to understanding the unique benefits and challenges of our DES system but also holds promise for advancing materials in the field of energy, paving the way for future developments in advanced energy materials.

4. Conclusion

To sum up, the intermolecular interaction of DES were investigated via the DFT+D3 calculations. The results of quantum chemical properties from DFT+D3 calculations indicate the DES conformer (i) where chloride ion in the center interact with EG and choline is the most stable conformer that other

conformers (a) to (h). Moreover, chloride ion acts as a hydrogen bond acceptor and interacts with acidic hydrogen atoms of EG as well after mixing ChCl with EG as a DES components. In detail, the primary interactions in DES conformer (i) are formed as follows: i) between the choline and chloride charge centers, ii) between the choline and EG, and iii) between the EG and the chloride anion.

Acknowledgments

References

[1]. J. Hao, X. Li, S. Yu, et al., *J. Energy Chem.* 24 (2015) 199–206. DOI: 10.1002/er.4096

[2]. B. Myrzakhmetov, A. Akhmetova, A. Bissenbay, et al., *Royal Society Open Science* 10 (2023) 230843. DOI: 10.1098/rsos.230843

[3]. K. Hooshyari, M. Javanbakht, M. Adibi, *Elecrochem. Acta* 205 (2016) 142–152. DOI: 10.1016/j.electacta.2016.04.115.

[4]. F.S. Ghareh Bagh, F.S. Mjalli, M.A. Hashim, et al., *J. Chem. Eng. Data* 58 (2013) 2154–2162. DOI: 10.1021/je400045d

[5]. G.R. Jenkin, A.Z. Al-Bassam, R.C. Harris, et al., *Miner. Eng.* 87 (2016) 18–24. DOI: 10.1016/j.mineng.2015.09.026

[6]. A.P. Abbott, G. Capper, K.J. McKenzie, K.S. Ryder, *J. Electroanal. Chem.* 599 (2007) 288–294. DOI: 10.1016/j.jelechem.2006.04.024

[7]. G. Garcia, M. Atilhan, S. Aparicio, *J. Phys. Chem. C* 119 (2015) 21413–21425. DOI: 10.1021/acs.jpcc.5b04585

[8]. C. Florindo, F.S. Oliveira, L.P.N. Rebelo, et al., *ACS Sustain. Chem. Eng.* 2 (2014) 2416–2425. DOI: 10.1021/sc500439w

[9]. E. Durand, J. Lecomte, P. Villeneuve, *Eur. J. Lipid Sci. Tech.* 115 (2016) 379–385. DOI: 10.1002/ejlt.201200416

[10]. B. Jiang, H. Dou, L. Zhang, et al., *J. Membr. Sci.* 536 (2017) 123–132. DOI: 10.1016/j.memsci.2017.05.004

[11]. E.S.C. Ferreira, I.V. Voroshylova, N.M. Figueiredo, M.N.D.S. Cordeiro, *J. Chem. Phys.* 155 (2021) 064506. DOI: 10.1063/5.0058561

[12]. B. Doherty, O. Acevedo, *J. Phys. Chem. B* 122 (2018) 9982–9993. DOI: 10.1021/acs.jpcb.8b06647

[13]. J.P Bittner, I. Smirnova, S. Jakobtorweihen, *Molecules* 29 (2024) 703. DOI: 10.3390/molecules29030703

[14]. M. Karibayev, D. Bekeshov, B. Myrzakhmetov, et al., *Eurasian Chem.-Technol. J.* 25 (2023) 89–102. DOI: 10.18321/ectj1499

[15]. M.Q. Farooq, N.M. Abbasi, J.L. Anderson, *J. Chromatogr. A* 1633 (2020) 461613. DOI: 10.1016/j.chroma.2020.461613.

[16]. V. Migliorati, F. Sessa, P. D'Angelo, *Chem. Phys. Lett.* 737 (2019) 100001. DOI: 10.1016/j.cpletx.2018.100001

[17]. R. Svigelj, R. Toniolo, C. Bertoni, A. Fraleoni-Morgera, *Sensors* 24 (2024) 2403. DOI: 10.3390/s24082403.

[18]. D. Carriazo, M.C. Serrano, M.C. Gutiérrez, et al., *Chem. Soc. Rev.* 41 (2012) 4996–5014. DOI: 10.1039/C2CS15353J

[19]. S. Zahn, B. Kirchner, D. Mollenhauer, *ChemPhysChem* 17 (2016) 3354–3358. DOI: 10.1002/cphc.201600348

[20]. P.J. Stephens, F.J. Devlin, C.F. Chabalowski, M.J. Frisch, *J. Phys. Chem.* 98 (1994) 11623–11627. DOI: 10.1021/j100096a001

[21]. B. Mennucci, *WIREs Comput. Mol. Sci.* 2 (2012) 386–404. DOI: 10.1002/wcms.1086

[22]. P.M. Gill, B.G. Johnson, J.A. Pople, M.J. Frisch, *Chem. Phys. Lett.* 197 (1992) 499–505. DOI: 10.1016/0009-2614(92)85807-M

[23]. E. De Castro, F. Jorge, *J. Chem. Phys.* 108 (1998) 5225–5229. DOI: 10.1063/1.475959

[24]. M. Frisch, G. Trucks, H. Schlegel, G. Scuseria, M. Robb, J. Cheeseman, G. Scalmani, V. Barone, G. Petersson, H. Nakatsuji, et al., G16 c01. gaussian 16, revision c. 01, gaussian, Inc., Wallin 248 (2016).

[25]. T. Lu, F. Chen, *J. Comput. Chem.* 33 (2012) 580–592. DOI: 10.1002/jcc.22885.16

[26]. C. Carlesi, R.C. Harris, A.P. Abbott, G.R. Jenkin, *Minerals* 12 (2022) 65. DOI: 10.3390/min12010065

[27]. R.B. Leron, M.H. Li, *Thermochim. Acta* 551 (2013) 14–19. DOI: 10.1016/j.tca.2012.09.041

[28]. F. Gabriele, M. Chiarini, R. Germani, et al., *J. Mol. Liq.* 291 (2019) 111301. DOI: 10.1016/j.molliq.2019.111301

[29]. D. Lapena, L. Lomba, M. Artal, et al., *Fluid Ph. Equilibria* 492 (2019) 1–9. DOI: 10.1016/j.fluid.2019.03.018

[30]. S.L. Perkins, P. Painter, C.M. Colina, *J. Chem. Eng. Data* 59 (2014) 3652–3662. DOI: 10.1021/je500520h.

[31]. N. Peeters, K. Janssens, D. de Vos, et al., *Green Chem.* 24 (2022) 6685–6695. DOI: 10.1039/D2GC02075K

[32]. C.Y. Wong, W.Y. Wong, R. Walvekar, et al., *J. Mol. Liq.* 269 (2018) 675–683. DOI: 10.1016/j.molliq.2018.08.102

[33]. M. Zhong, Q.F. Tang, Y.W. Zhu, et al., *J. Power Sources* 452 (2020) 227847. DOI: 10.1016/j.jpowsour.2020.227847